Supplement of Atmos. Chem. Phys., 18, 6141–6156, 2018
https://doi.org/10.5194/acp-18-6141-2018-supplement

Atmospheric Chemistry and Physics
Open Access
EGU

Supplement of

Impacts of air pollutants from fire and non-fire emissions on the regional air quality in Southeast Asia

Hsiang-He Lee et al.

Correspondence to: Hsiang-He Lee (hsiang-he@smart.mit.edu)

S1. Uncertainty analysis of modeled LVDs

Since a full-scale forward-integrating uncertainty analysis based on WRF-Chem model would extremely expensive computationally, we have adopted a method for dichotomous (yes or no LVDs) cases and then give a contingency table (Table S6) to address model evaluation and to quantify model performance.

We have estimated *accuracy* based on the Eq. (S1):

$$Accuracy = \frac{hits+correct\ negatives}{hits+misses+false\ alarms+correct\ negatives} \quad \text{(S1)}$$

Accuracy here is also called fraction correct, which is easy to evaluate model prediction. However, it can be misleading for some cases since it is heavily influenced by the most common category, usually "no event" in the case of LVD. Hence, we have provided *threat score* in this study as well. Based on the equation of threat score (or critical success index), we can measure the fraction of observed and/or modeled LVDs that were correctly predicted. Threat score also can be referred as the *accuracy* when correct negatives have been removed from consideration, that is, threat score only concerns modeled LVDs that count.

$$Threat\ Score = \frac{hits}{hits+misses+false\ alarms} \quad \text{(S2)}$$

Figure S8 shows the mean value of accuracy and threat score of modeled LVDs among 50 ASEAN cities in three experiments: FF, BB, and FFBB. Since the category of correct negatives is heavily counted in the accuracy, the values are also twice as high as the threat scores. Basically, BB has the lowest threat score while FFBB has the highest score as expected.

S2. The impact of fire and non-fire aerosols on regional climate

Besides influencing surface and air temperature through scattering and absorbing solar radiation, aerosols can also alter the spatiotemporal patterns of precipitation via aerosol direct and indirect effects (Wang, 2015). Over the modeled domain, rainfall (in quantity) mainly comes from convective clouds. When the model is configured with a relatively coarse resolution as adopted in our study, however, the convective precipitation process is calculated through the cumulus parameterization of the model, which follows a mass-flux approach to diagnose rainfall and does not interact with aerosols. Despite of this drawback, aerosols can still influence the radiation budget through their direct effect. The thermodynamic consequences of this effect can further influence the cloud formation. On the other hand, the model does contain aerosol-cloud microphysical interaction for stratiform clouds; therefore, aerosols can influence these clouds through the so-called indirect effects by providing cloud condensation nuclei for cloud droplets to form. Hence, cumulus rainfall can be still affected indirectly through dynamical and thermodynamic processes initiated by either aerosol direct effects, indirect effects in stratiform clouds, or both.

By comparing the precipitation in FF and FFBB, we have examined the impact of the extra forcing from fire aerosols on precipitation in the modeled Southeast Asia domain (10°S-20°N in latitude, 90°E–150°E in longitude). Non-fire aerosols provide a baseline pattern because of the persistency of fossil fuel emissions, while biomass burning emissions load additional aerosols in the air to alter total aerosol radiative forcing, which then would change precipitation. Through aerosol direct and indirect effects, the difference of monthly regional mean downward shortwave radiation at surface is 8.8 W m^{-2} (232.6 W m^{-2} in FF versus 223.8 W m^{-2} in FFBB; Fig. S9). The data are calculated over land only. Owing to

the reduction of surface incoming solar radiation by fire aerosols, surface skin temperature is 0.2 K lower in FFBB than in FF (Fig. S10). Lower surface temperature brought by fire aerosols would suppress convection (Berg et al., 2013). As a result, the model produced a lower monthly regional mean precipitation in FFBB than in FF by 0.2 mm day^{-1} over land (11.15 mm day^{-1} versus 11.35 mm day^{-1}; Fig. S11), with the most substantial rainfall changes occurring in the fire emission regions of Sumatra and Borneo. We also find higher cloud water mass in FFBB, which has stronger radiative forcing than aerosols. Nevertheless, further study using a cloud-resolving simulation is necessary.

Table S1. Equations for the calculation of 24-hr average PM_{10} concentration ($\mu g\ m^{-3}$) based on Air Quality Index (AQI) number obtained from the website of Ministry of Natural Resources and Environment, Department of Environment, Malaysia (Malaysia, 2000).

AQI	Equation
0 - 50	$PM_{10} = AQI$
51 – 100	$PM_{10} = (AQI-50)\times2+50$
101 – 200	$PM_{10} = (AQI-100)\times2+150$
201 – 300	$PM_{10} = (AQI-200)/1.4286+350$
301 – 400	$PM_{10} = (AQI-300)/1.25+420$
401 – 500	$PM_{10} = (AQI-400)+500$

Table S2. Sampling period of Surface PARTiculate mAtter Network (SPARTAN) stations in Southeast Asia and available compositional features.

	Available period	**Composition**
Hanoi	May 2015 – present	$PM_{2.5}$, Ammoniated Sulfate, Ammonium Nitrate, Crustal Material, Residual Material, Sea Salt, Equivalent Black Carbon, Trace Element Oxides, Particle-Bound Water (RH=0.35)
Singapore	July 2015 – present	
Bandung	January 2014 – present	
Manila	February 2014 – present	

Table S3. Mean annual emissions and modeled concentration of BC, OC, SO_2, CO and NO_2 from 2006 REAS and EDGAR emission inventories in the simulated domain.

	REAS		EDGAR	
	Emissions (Tg/year)	Modeled conc. (ug/m^3 or ppmv)	Emissions (Tg/year)	Modeled conc. (ug/m^3 or ppmv)
OC	0.12	0.1131	0.15	0.1487
BC	0.036	0.0311	0.065	0.0643
SO_2	0.43	1.03×10^{-4}	0.65	2.01×10^{-4}
NO_2	0.3	4.94×10^{-4}	0.205	4.83×10^{-4}
CO	3.53	8.10×10^{-2}	7.48	8.72×10^{-2}

Table S4. Comparison of the Air Quality Index (AQI) values with level of pollution index category and breakpoints for AQI derived from modeled 24-hr $PM_{2.5}$ (μg m^{-3}) and modeled 9-hr O_3 (ppb).

Index Category	AQI	24-hr $PM_{2.5}$ (μg/m^3)	9-hr O_3 (ppb)
Good	0 - 50	0.0 – 12.0	0 – 59
Moderate	51 – 100	12.1 – 35.4	60 – 75
Unhealthy	101 – 200	35.5 – 150.4	76 – 115
Very Unhealthy	201 – 300	150.5 – 250.4	116 – 374
Hazardous	301 – 400	250.5 – 350.4	/
Hazardous	401 – 500	350.5 – 500.4	/

Table S5. Features are used to train Machine Learning algorithms for Changi, Seletar and Paya Labar data.

Features for Changi	Features for Seletar and Paya Labar
Hotspot count in mainland Southeast Asia (HS_M)	Hotspot count in mainland Southeast Asia (HS_M)
Hotspot count in Sumatra (HS_S)	Hotspot count in Sumatra (HS_S)
Hotspot count in Borneo (HS_B)	Hotspot count in Borneo (HS_B)
Month (Month)	Month (Month)
Wind direction (WD)	Wind direction (WD)
Weather condition[a] (SRV)	Weather condition[a] (SRV)
Classified precipitation[b] (PPT)	Classified wind speed[c] (WS)
Classified wind speed[c] (WS)	Classified relative humidity[d] (RH)
Classified relative humidity[d] (RH)	5-day continuous rainfall in mainland Southeast Asia (5PPT_M)
Classified pressure[e] (Pres)	5-day continuous rainfall in Sumatra (5PPT_S)
Classified dew point[f] (Dtemp)	5-day continuous rainfall in Borneo (5PPT_B)
Classified temperature[g] (Temp)	10-day continuous rainfall in mainland Southeast Asia (10PPT_M)
5-day continuous rainfall in mainland Southeast Asia (5PPT_M)	10-day continuous rainfall in Sumatra (10PPT_S)
5-day continuous rainfall in Sumatra (5PPT_S)	10-day continuous rainfall in Borneo (10PPT_B)
5-day continuous rainfall in Borneo (5PPT_S)	
10-day continuous rainfall in mainland Southeast Asia (10PPT_M)	
10-day continuous rainfall in Sumatra (10PPT_S)	
10-day continuous rainfall in Borneo (10PPT_B)	

[a]Based on Allwine and Whiteman (1994) to classify weather condition to recirculation, ventilation, and stagnation.
[b]Precipitation has been classified into 3 categories and the breakpoints are 0 and 100 mm day^{-1}.
[c]Wind speed has been classified into 3 categories and the breakpoints are 5 and 10 m sec^{-1}.
[d]Relative humidity has been classified into 4 categories and the breakpoints are 70, 80, and 90%.
[e]Pressure has been classified into 3 categories and the breakpoints are 1005 and 1010 mb.
[f]Dew point has been classified into 3 categories and the breakpoints are 24 and 26°C.
[g]Temperature has been classified into 4 categories and the breakpoints are 25, 27.8, and 29°C.

Table S6. Contingency table for dichotomous (yes or no LVDs) cases

		Observed LVD	
		yes	no
Modeled LVD	yes	***hits***	***false alarms***
	no	***misses***	***correct negatives***

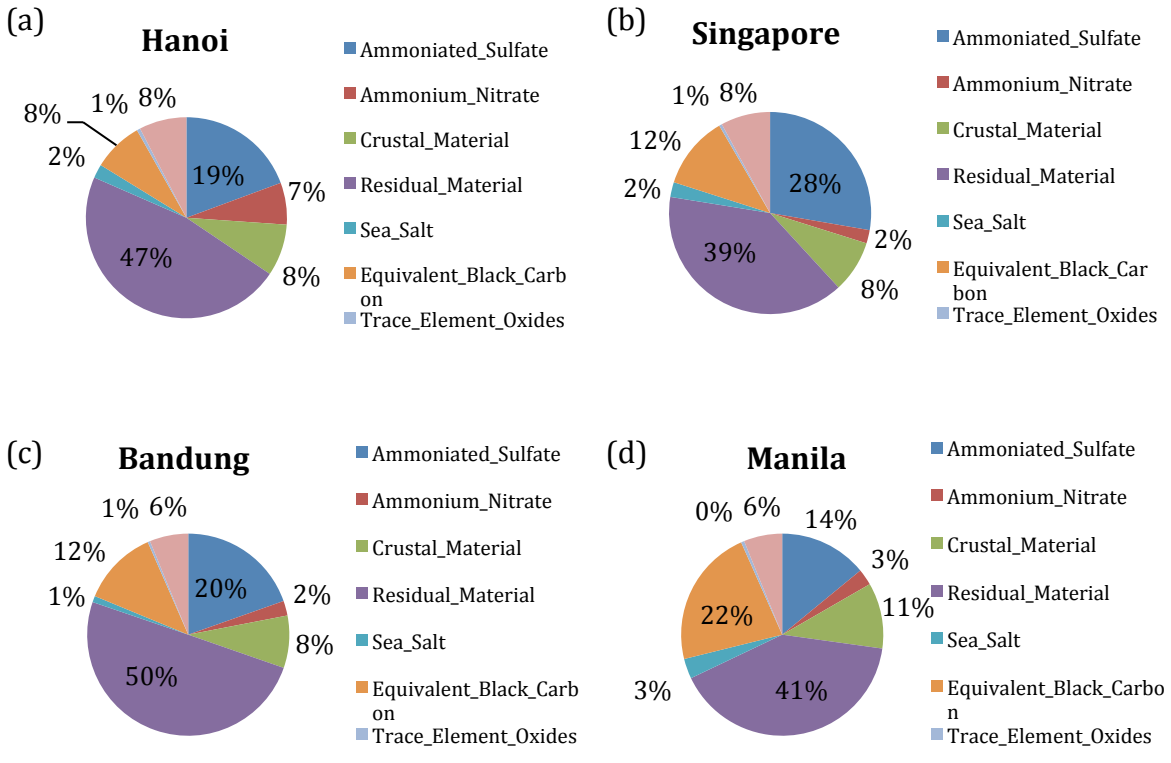

Figure S1. Pie chart of chemical components of $PM_{2.5}$ from the Surface PARTiculate mAtter Network (SPARTAN) filter samples in (a) Hanoi (Vietnam), (b) Singapore (Singapore), (c) Bandung (Indonesia), and (d) Manila (Philippines).

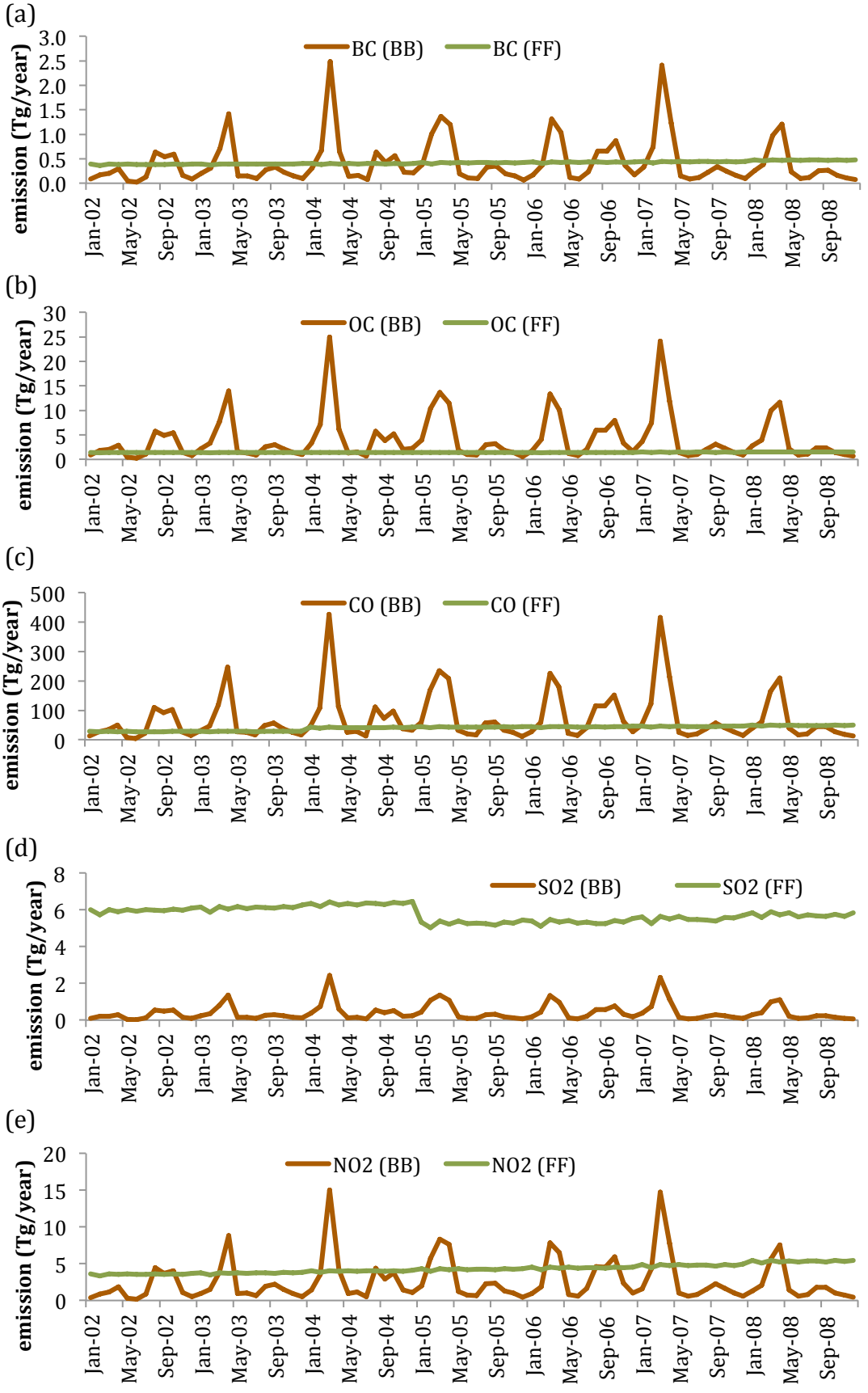
(a)
BC (BB)
BC (FF)
emission (Tg/year)
3.0
2.5
2.0
1.5
1.0
0.5
0.0
(b)
OC (BB)
OC (FF)
emission (Tg/year)
30
25
20
15
10
5
0
(c)
CO (BB)
CO (FF)
emission (Tg/year)
500
400
300
200
100
0
(d)
SO2 (BB)
SO2 (FF)
emission (Tg/year)
8
6
4
2
0
(e)
NO2 (BB)
NO2 (FF)
emission (Tg/year)
20
15
10
5
0
Jan-02
May-02
Sep-02
Jan-03
May-03
Sep-03
Jan-04
May-04
Sep-04
Jan-05
May-05
Sep-05
Jan-06
May-06
Sep-06
Jan-07
May-07
Sep-07
Jan-08
May-08
Sep-08

Figure S2. Time serious of domain averaged monthly (a) black carbon (BC), (b) organic carbon (OC), (c) carbon monoxide (CO), (d) sulfur dioxide (SO_2) and (e) nitrogen dioxide (NO_2) emission (Tg $year^{-1}$) from biomass burning (BB; red lines) and fossil fuel (FF; green lines) emission inventories during 2002-2008.

Cities	Country	2002	2003	2004	2005	2006	2007	2008
Jakarta	Indonesia	801 (121-1594)	804 (115-1606)	856 (135-1693)	902 (153-1766)	841 (113-1692)	922 (147-1819)	943 (150-1859)
Bangkok	Thailand	718 (55-1722)	733 (55-1766)	541 (0-1508)	782 (59-1886)	879 (76-2068)	797 (53-1961)	753 (39-1909)
Ho Chi Minh City	Vietnam	0 (0-0)	0 (0-0)	0 (0-0)	0 (0-0)	0 (0-0)	0 (0-0)	0 (0-0)
Hanoi	Vietnam	381 (28-835)	424 (39-902)	444 (42-942)	421 (30-926)	452 (36-984)	460 (36-1006)	927 (90-1965)
Singapore	Singapore	0 (0-0)	0 (0-0)	0 (0-0)	0 (0-0)	0 (0-0)	0 (0-0)	0 (0-0)
Yangon	Myanmar	0 (0-0)	0 (0-0)	0 (0-0)	0 (0-0)	0 (0-0)	0 (0-0)	0 (0-0)
Surabaya	Indonesia	197 (19-416)	193 (17-415)	214 (23-445)	216 (23-451)	207 (19-444)	220 (22-464)	214 (19-459)
Quezon City	Philippines	0 (0-0)	0 (0-0)	0 (0-0)	0 (0-0)	0 (0-0)	0 (0-0)	0 (0-0)
Bandung	Indonesia	193 (25-392)	189 (22-388)	203 (27-410)	215 (31-429)	180 (16-387)	216 (29-435)	212 (25-432)
Bekasi	Indonesia	145 (18-296)	152 (18-311)	169 (23-340)	184 (27-367)	169 (18-353)	197 (27-395)	205 (28-412)
Medan	Indonesia	0 (0-0)	0 (0-0)	0 (0-0)	0 (0-0)	0 (0-0)	0 (0-0)	0 (0-0)
Tangerang	Indonesia	116 (17-230)	121 (17-241)	134 (21-264)	146 (25-285)	140 (19-282)	159 (25-313)	167 (27-330)
Hai Phong	Vietnam	0 (0-0)	0 (0-0)	0 (0-0)	0 (0-0)	0 (0-0)	0 (0-0)	0 (0-0)
Depok	Indonesia	123 (28-230)	128 (28-243)	142 (32-267)	158 (38-294)	157 (33-299)	176 (40-328)	183 (41-345)
Manila	Philippines	0 (0-0)	0 (0-0)	0 (0-0)	0 (0-0)	0 (0-0)	0 (0-0)	0 (0-0)
Semarang	Indonesia	119 (19-235)	120 (18-239)	132 (23-258)	139 (25-270)	136 (21-269)	142 (23-280)	149 (25-293)
Palembang	Indonesia	0 (0-0)	0 (0-0)	0 (0-0)	0 (0-0)	0 (0-0)	0 (0-0)	0 (0-0)
Caloocan	Philippines	0 (0-0)	0 (0-0)	0 (0-0)	0 (0-0)	0 (0-0)	0 (0-0)	0 (0-0)
Kuala Lumpur	Malaysia	0 (0-205)	0 (0-119)	0 (0-165)	0 (0-214)	0 (0-178)	0 (0-224)	0 (0-227)
Davao City	Philippines	0 (0-0)	0 (0-0)	0 (0-0)	0 (0-0)	0 (0-0)	0 (0-0)	0 (0-0)
South Tangerang	Indonesia	120 (18-239)	119 (17-237)	125 (20-246)	130 (22-254)	119 (16-240)	129 (21-254)	130 (21-256)
Makassar	Indonesia	0 (0-0)	0 (0-0)	0 (0-0)	0 (0-0)	0 (0-0)	0 (0-0)	0 (0-0)
Phnom Penh	Cambodia	0 (0-0)	0 (0-0)	0 (0-0)	0 (0-0)	0 (0-0)	0 (0-0)	0 (0-0)
Can Tho	Vietnam	0 (0-229)	0 (0-236)	0 (0-230)	0 (0-233)	0 (0-269)	51 (0-291)	131 (0-329)
Batam	Indonesia	0 (0-0)	0 (0-0)	0 (0-0)	0 (0-0)	0 (0-0)	0 (0-0)	0 (0-0)
Pekan Baru	Indonesia	0 (0-0)	0 (0-0)	0 (0-0)	0 (0-0)	0 (0-0)	0 (0-0)	0 (0-0)
Bogor	Indonesia	96 (22-179)	94 (21-179)	99 (23-186)	105 (25-196)	100 (21-190)	107 (25-200)	108 (24-202)
Da Nang	Vietnam	0 (0-0)	0 (0-0)	0 (0-0)	0 (0-0)	0 (0-0)	0 (0-0)	0 (0-0)
Bien Hoa	Vietnam	0 (0-0)	0 (0-0)	0 (0-0)	0 (0-0)	0 (0-0)	0 (0-0)	0 (0-0)
Bandar Lampung	Indonesia	64 (8-130)	64 (8-131)	67 (8-136)	66 (7-137)	73 (9-147)	68 (7-143)	76 (9-154)
Johor Bahru	Malaysia	0 (0-0)	0 (0-0)	0 (0-0)	0 (0-0)	0 (0-0)	0 (0-0)	0 (0-0)
Mandalay	Myanmar	0 (0-0)	0 (0-0)	0 (0-0)	0 (0-0)	0 (0-0)	0 (0-0)	0 (0-0)
Padang	Indonesia	0 (0-0)	0 (0-0)	0 (0-0)	0 (0-0)	0 (0-0)	0 (0-0)	0 (0-0)
Cebu City	Philippines	0 (0-0)	0 (0-0)	0 (0-0)	0 (0-0)	0 (0-0)	0 (0-0)	0 (0-0)
Denpasar	Indonesia	0 (0-0)	0 (0-0)	0 (0-0)	0 (0-0)	0 (0-0)	0 (0-0)	0 (0-0)
Malang	Indonesia	0 (0-0)	0 (0-0)	0 (0-74)	0 (0-75)	0 (0-39)	0 (0-68)	0 (0-61)
Samarinda	Indonesia	0 (0-0)	0 (0-0)	0 (0-0)	0 (0-0)	0 (0-0)	0 (0-0)	0 (0-0)
Zamboanga City	Philippines	0 (0-0)	0 (0-0)	0 (0-0)	0 (0-0)	0 (0-0)	0 (0-0)	0 (0-0)
George Town	Malaysia	66 (0-208)	0 (0-167)	30 (0-193)	90 (4-223)	0 (0-178)	43 (0-198)	62 (0-206)
Ipoh	Malaysia	0 (0-0)	0 (0-0)	0 (0-0)	0 (0-0)	0 (0-0)	0 (0-0)	0 (0-0)
Taguig	Philippines	0 (0-0)	0 (0-0)	0 (0-0)	0 (0-0)	0 (0-0)	0 (0-0)	0 (0-0)
Tasikmalayu	Indonesia	31 (3-65)	30 (3-65)	34 (3-73)	41 (5-83)	36 (3-78)	43 (5-90)	44 (4-92)
Antipolo	Philippines	0 (0-0)	0 (0-0)	0 (0-0)	0 (0-0)	0 (0-0)	0 (0-0)	0 (0-0)
Banjarmasin	Indonesia	0 (0-0)	0 (0-0)	0 (0-0)	0 (0-0)	0 (0-0)	0 (0-0)	0 (0-0)
Shah Alam	Malaysia	0 (0-91)	0 (0-52)	0 (0-71)	0 (0-90)	0 (0-73)	0 (0-90)	0 (0-90)
Pasig	Philippines	0 (0-0)	0 (0-0)	0 (0-0)	0 (0-0)	0 (0-0)	0 (0-0)	0 (0-0)
Balikpapan	Indonesia	0 (0-0)	0 (0-0)	0 (0-0)	0 (0-0)	0 (0-0)	0 (0-0)	0 (0-0)
Serang	Indonesia	44 (9-85)	44 (8-85)	45 (9-86)	45 (9-87)	45 (8-87)	45 (8-88)	46 (9-89)
Petaling Jaya	Malaysia	0 (0-87)	0 (0-50)	0 (0-68)	0 (0-86)	0 (0-70)	0 (0-87)	0 (0-86)
Kuching	Malaysia	0 (0-0)	0 (0-0)	0 (0-0)	0 (0-0)	0 (0-0)	0 (0-0)	0 (0-0)

Figure S3. Premature mortality in different years from 2002 to 2008 and cities in Association of Southeast Asian Nations (ASEAN) due to exposures $PM_{2.5}$ in FF (95% confidence intervals). Colors from green to red represent relative number scale.

Cities	Country	2002	2003	2004	2005	2006	2007	2008
Jakarta	Indonesia	0 (0-0)	0 (0-0)	0 (0-0)	0 (0-0)	0 (0-0)	0 (0-0)	0 (0-0)
Bangkok	Thailand	0 (0-1058)	744 (57-1784)	829 (73-1941)	931 (95-2133)	776 (54-1901)	907 (78-2138)	828 (55-2037)
Ho Chi Minh City	Vietnam	0 (0-0)	0 (0-0)	428 (0-1452)	0 (0-965)	0 (0-0)	0 (0-0)	0 (0-0)
Hanoi	Vietnam	0 (0-0)	21 (0-697)	0 (0-661)	122 (0-769)	0 (0-648)	344 (0-905)	668 (0-1709)
Singapore	Singapore	0 (0-0)	0 (0-0)	0 (0-0)	0 (0-0)	0 (0-0)	0 (0-0)	0 (0-0)
Yangon	Myanmar	0 (0-0)	14 (0-452)	289 (20-645)	243 (11-589)	0 (0-331)	333 (25-728)	125 (0-559)
Surabaya	Indonesia	0 (0-0)	0 (0-0)	0 (0-0)	0 (0-0)	0 (0-0)	0 (0-0)	0 (0-0)
Quezon City	Philippines	0 (0-0)	0 (0-0)	0 (0-0)	0 (0-0)	0 (0-0)	0 (0-0)	0 (0-0)
Bandung	Indonesia	0 (0-0)	0 (0-0)	0 (0-0)	0 (0-0)	0 (0-0)	0 (0-0)	0 (0-0)
Bekasi	Indonesia	0 (0-0)	0 (0-0)	0 (0-0)	0 (0-0)	0 (0-0)	0 (0-0)	0 (0-0)
Medan	Indonesia	0 (0-0)	0 (0-0)	0 (0-0)	0 (0-0)	0 (0-0)	0 (0-0)	0 (0-0)
Tangerang	Indonesia	0 (0-0)	0 (0-0)	0 (0-0)	0 (0-0)	0 (0-0)	0 (0-0)	0 (0-0)
Hai Phong	Vietnam	0 (0-0)	0 (0-0)	0 (0-0)	0 (0-0)	0 (0-0)	0 (0-341)	0 (0-338)
Depok	Indonesia	0 (0-0)	0 (0-0)	0 (0-0)	0 (0-139)	0 (0-0)	0 (0-0)	0 (0-0)
Manila	Philippines	0 (0-0)	0 (0-0)	0 (0-0)	0 (0-0)	0 (0-0)	0 (0-0)	0 (0-0)
Semarang	Indonesia	0 (0-0)	0 (0-0)	0 (0-0)	0 (0-0)	0 (0-0)	0 (0-0)	0 (0-0)
Palembang	Indonesia	92 (8-199)	0 (0-0)	89 (6-199)	0 (0-0)	145 (29-279)	0 (0-0)	0 (0-0)
Caloocan	Philippines	0 (0-0)	0 (0-0)	0 (0-0)	0 (0-0)	0 (0-0)	0 (0-0)	0 (0-0)
Kuala Lumpur	Malaysia	0 (0-0)	0 (0-0)	108 (4-264)	117 (6-278)	106 (2-269)	0 (0-0)	0 (0-0)
Davao City	Philippines	0 (0-0)	0 (0-0)	0 (0-0)	0 (0-0)	0 (0-0)	0 (0-0)	0 (0-0)
South Tangerang	Indonesia	0 (0-0)	0 (0-0)	0 (0-0)	0 (0-0)	0 (0-0)	0 (0-0)	0 (0-0)
Makassar	Indonesia	0 (0-0)	0 (0-0)	0 (0-0)	0 (0-0)	0 (0-0)	0 (0-0)	0 (0-0)
Phnom Penh	Cambodia	0 (0-0)	8 (0-58)	44 (5-93)	36 (2-82)	36 (2-84)	40 (3-91)	39 (2-91)
Can Tho	Vietnam	0 (0-0)	0 (0-0)	54 (0-276)	0 (0-80)	0 (0-0)	0 (0-0)	0 (0-0)
Batam	Indonesia	0 (0-0)	0 (0-0)	0 (0-0)	0 (0-0)	0 (0-0)	0 (0-0)	0 (0-0)
Pekan Baru	Indonesia	0 (0-57)	0 (0-0)	53 (5-112)	81 (19-151)	75 (13-147)	62 (6-132)	70 (8-145)
Bogor	Indonesia	0 (0-0)	0 (0-0)	0 (0-0)	0 (0-92)	0 (0-0)	0 (0-0)	0 (0-0)
Da Nang	Vietnam	0 (0-0)	0 (0-0)	0 (0-157)	0 (0-0)	0 (0-0)	0 (0-0)	0 (0-0)
Bien Hoa	Vietnam	0 (0-0)	0 (0-0)	0 (0-94)	0 (0-0)	0 (0-0)	0 (0-0)	0 (0-0)
Bandar Lampung	Indonesia	0 (0-43)	0 (0-0)	0 (0-0)	0 (0-22)	0 (0-57)	0 (0-0)	0 (0-0)
Johor Bahru	Malaysia	0 (0-0)	0 (0-0)	0 (0-0)	0 (0-0)	0 (0-0)	0 (0-0)	0 (0-0)
Mandalay	Myanmar	0 (0-0)	270 (21-591)	310 (29-649)	273 (20-602)	284 (21-623)	345 (36-715)	316 (27-678)
Padang	Indonesia	0 (0-0)	0 (0-0)	0 (0-0)	0 (0-0)	58 (6-122)	0 (0-64)	0 (0-52)
Cebu City	Philippines	0 (0-0)	0 (0-0)	0 (0-0)	0 (0-0)	0 (0-0)	0 (0-0)	0 (0-0)
Denpasar	Indonesia	0 (0-0)	0 (0-0)	0 (0-0)	0 (0-0)	0 (0-0)	0 (0-0)	0 (0-0)
Malang	Indonesia	0 (0-0)	0 (0-0)	0 (0-0)	0 (0-0)	0 (0-0)	0 (0-0)	0 (0-0)
Samarinda	Indonesia	0 (0-0)	0 (0-0)	0 (0-0)	0 (0-0)	0 (0-0)	0 (0-0)	0 (0-0)
Zamboanga City	Philippines	0 (0-0)	0 (0-0)	0 (0-0)	0 (0-0)	0 (0-0)	0 (0-0)	0 (0-0)
George Town	Malaysia	0 (0-0)	0 (0-0)	40 (0-196)	0 (0-140)	0 (0-0)	0 (0-0)	0 (0-0)
Ipoh	Malaysia	0 (0-0)	0 (0-0)	0 (0-74)	0 (0-0)	0 (0-0)	0 (0-0)	0 (0-0)
Taguig	Philippines	0 (0-0)	0 (0-0)	0 (0-0)	0 (0-0)	0 (0-0)	0 (0-0)	0 (0-0)
Tasikmalayu	Indonesia	0 (0-0)	0 (0-0)	0 (0-0)	0 (0-0)	0 (0-0)	0 (0-0)	0 (0-0)
Antipolo	Philippines	0 (0-0)	0 (0-0)	0 (0-0)	0 (0-0)	0 (0-0)	0 (0-0)	0 (0-0)
Banjarmasin	Indonesia	47 (6-96)	0 (0-0)	53 (8-106)	0 (0-0)	55 (8-110)	0 (0-0)	0 (0-0)
Shah Alam	Malaysia	0 (0-0)	0 (0-0)	46 (2-113)	49 (2-117)	43 (1-111)	0 (0-0)	0 (0-0)
Pasig	Philippines	0 (0-0)	0 (0-0)	0 (0-0)	0 (0-0)	0 (0-0)	0 (0-0)	0 (0-0)
Balikpapan	Indonesia	0 (0-0)	0 (0-0)	0 (0-0)	0 (0-0)	0 (0-0)	0 (0-0)	0 (0-0)
Serang	Indonesia	0 (0-0)	0 (0-0)	0 (0-0)	0 (0-0)	0 (0-0)	0 (0-0)	0 (0-0)
Petaling Jaya	Malaysia	0 (0-0)	0 (0-0)	44 (2-108)	47 (2-112)	42 (1-106)	0 (0-0)	0 (0-0)
Kuching	Malaysia	41 (2-97)	0 (0-0)	49 (3-111)	0 (0-0)	62 (6-131)	0 (0-0)	0 (0-0)

Figure S4. Same as Fig. S3 but $PM_{2.5}$ in BB.

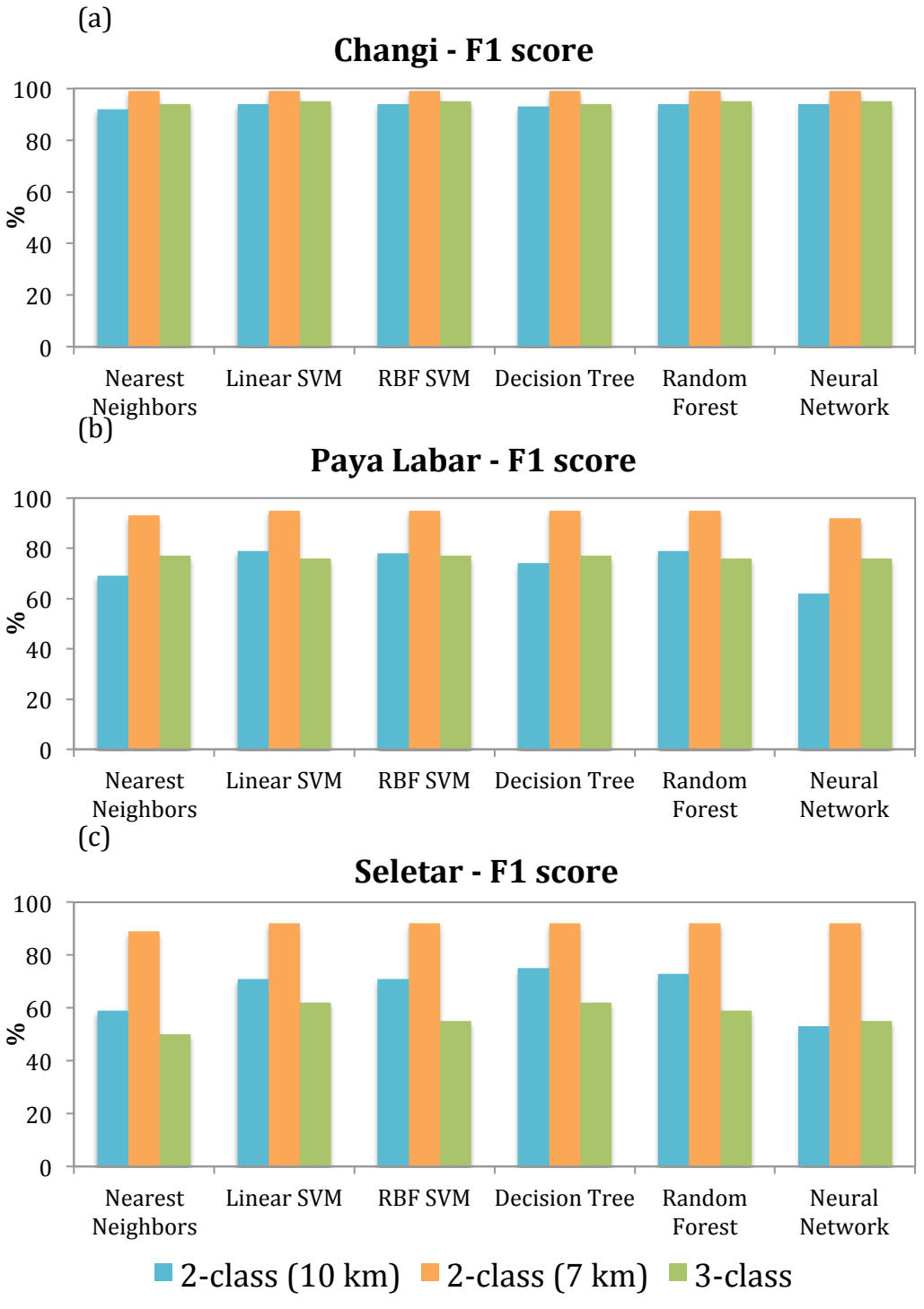

Figure S5. The F_1 score in 6 Machine Learning algorithms for two 2-class (7 km or 10 km visibility as a breakpoint) and one 3-class classifications haze prediction in (a) Changi, (b) Paya Labar, and (c) Seletar.

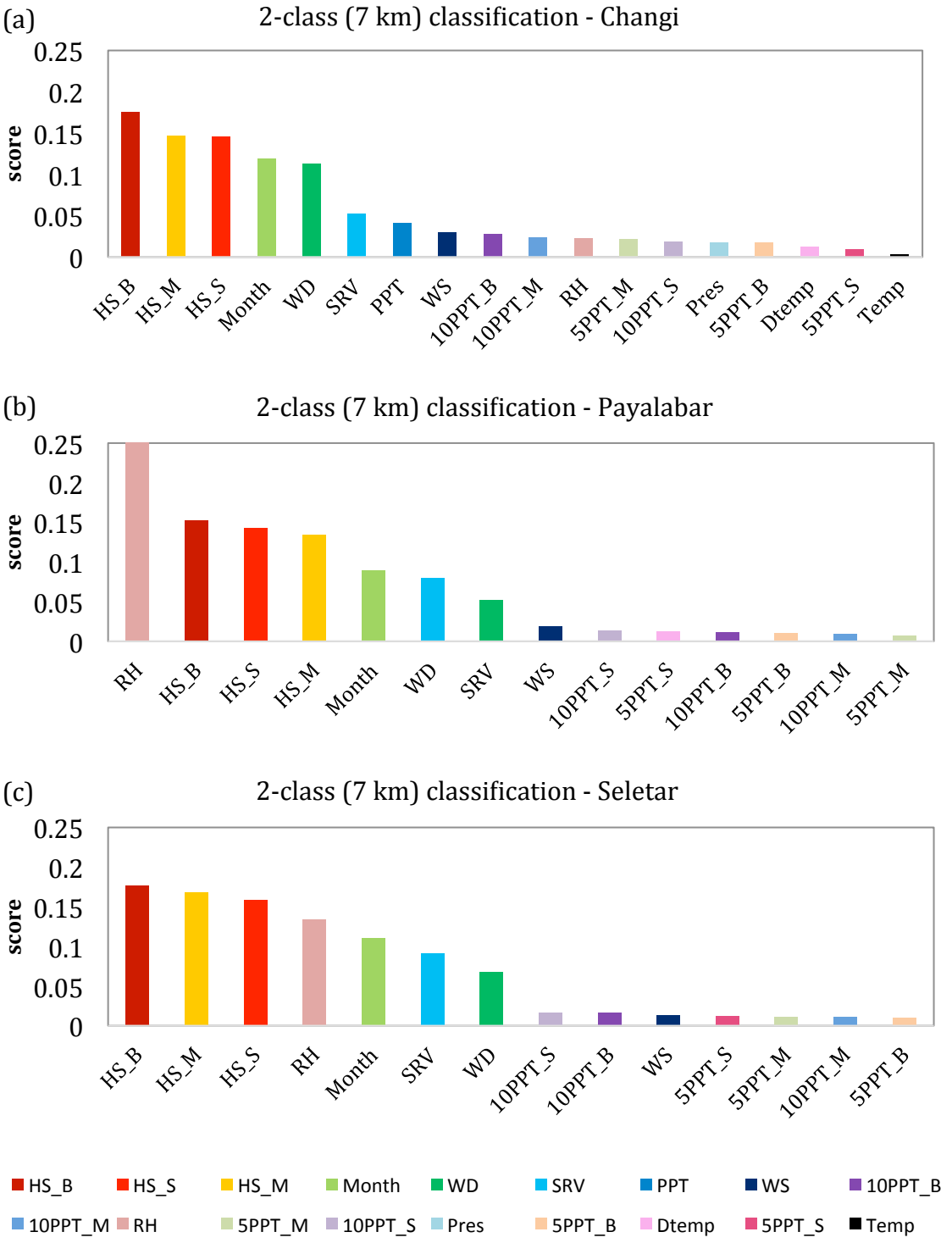

Figure S6. Feature importance by using 2-class classification Random Forest algorithm for (a) Changi, (b) Paya Labar, and (c) Seletar data. Desired outputs, haze versus non-haze events, are defined by using visibility 7 km as a breakpoint. Full name of each input feature are listed in Table S5.

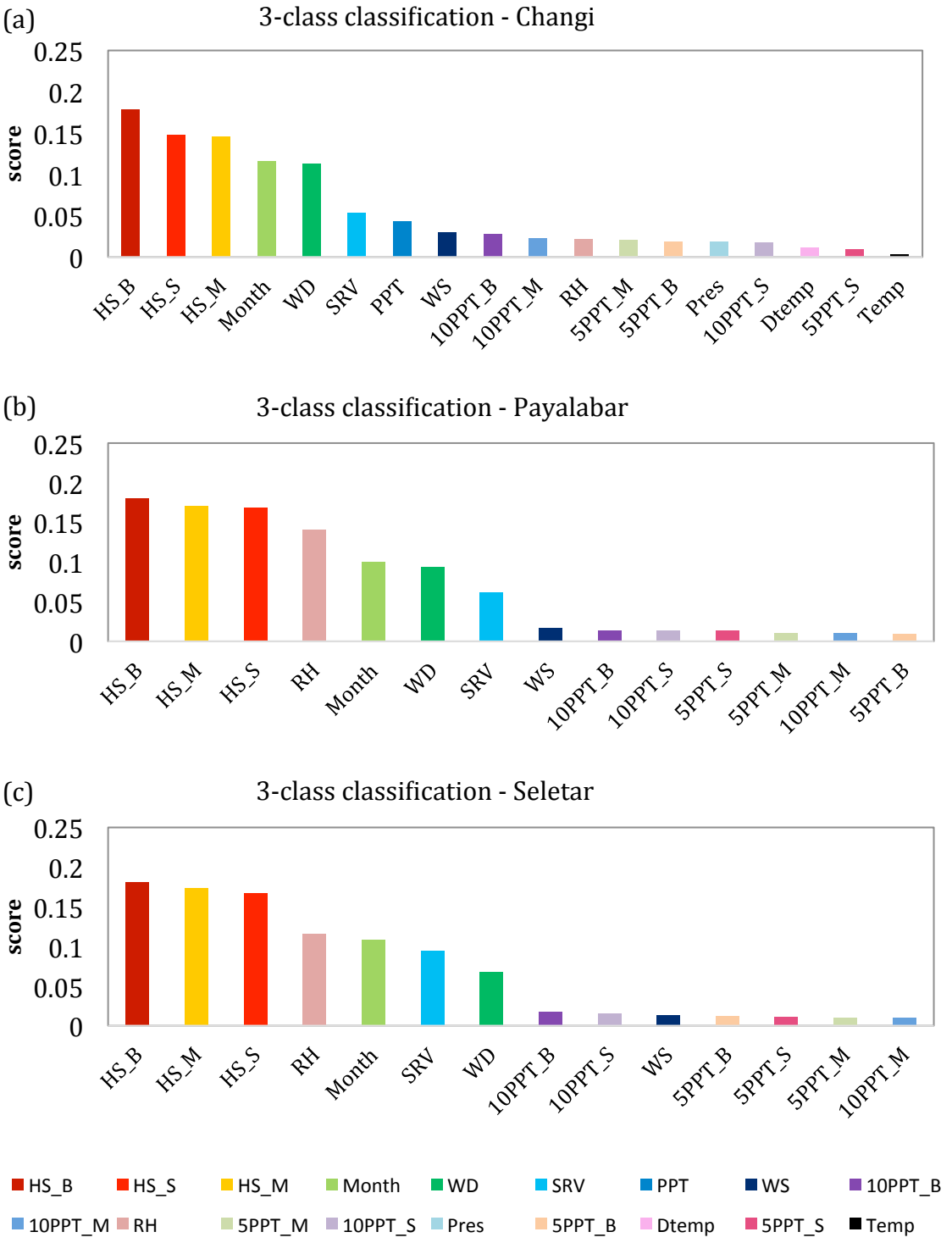

Figure S7. Feature importance by using 3-class classification Random Forest algorithm for (a) Changi, (b) Paya Labar, and (c) Seletar data. Desired outputs, severe haze, haze, and non-haze events, are defined by using visibility 7 and 10 km as breakpoints. Full name of each input feature are listed in Table S5.

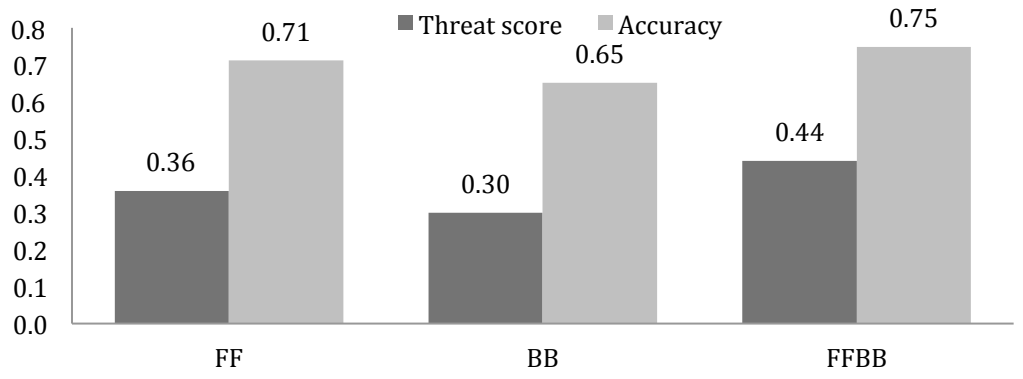

Figure S8. The mean value of accuracy and Threat score of modeled LVDs among 50 ASEAN cities in three experiment, FF, BB, and FFBB.

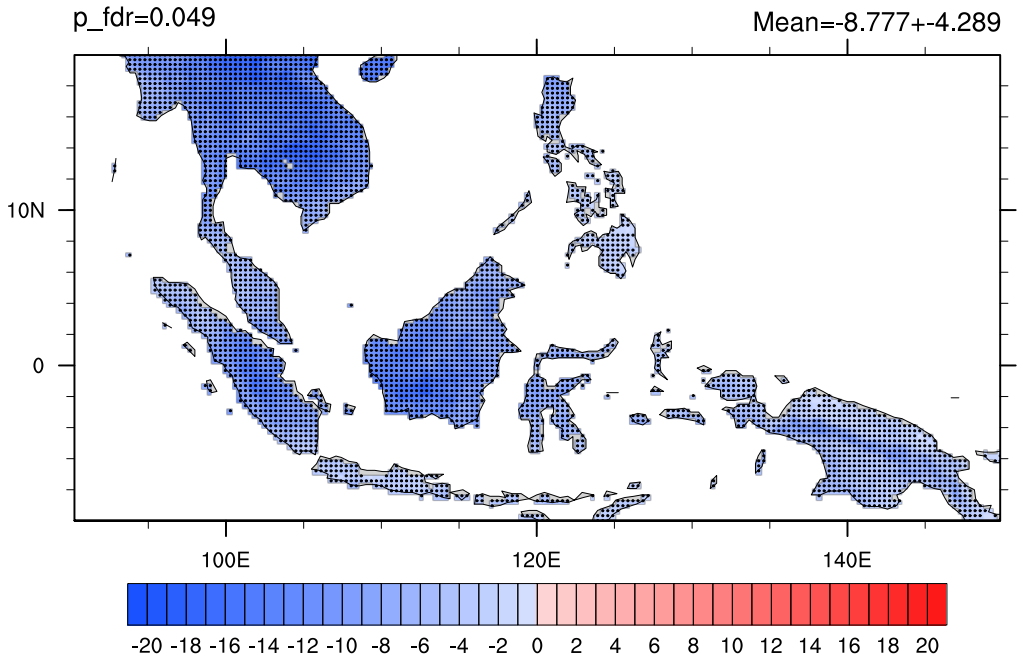

Figure S9. Total monthly mean downward shortwave radiation (W m^{-2}) between FFBB and FF (FFBB-FF) simulations during 2002–2008. Black dots indicate differences that are statistically significant at a significance level of α_{fdr} = 0.05 after controlling for the false discovery rate (FDR) (Benjamini and Hochberg, 1995; Wilks, 2016). The two-tailed p-values are generated by Welch's t-test, using monthly mean data as the input. The approximate p-value threshold, p_fdr, area mean and standard deviation (over land only) are recorded in the map above.

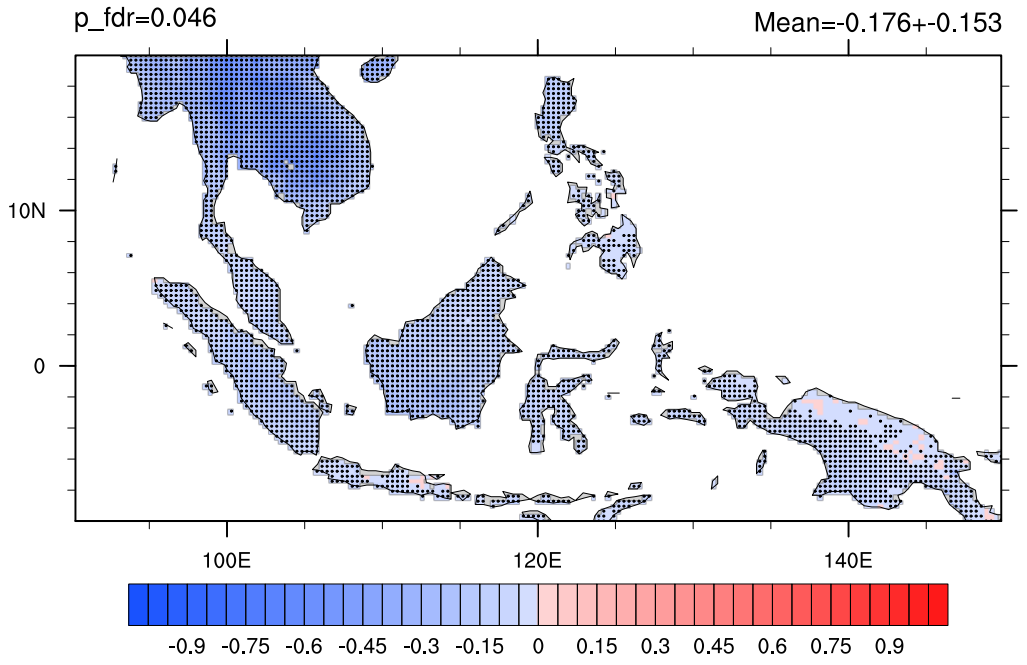

Figure S10. Total monthly mean surface skin temperature (K) between FFBB and FF (FFBB-FF) simulations during 2002–2008. Black dots indicate differences that are statistically significant at a significance level of $\alpha_{fdr} = 0.05$ after controlling for the false discovery rate (FDR) (Benjamini and Hochberg, 1995; Wilks, 2016). The two-tailed p-values are generated by Welch's t-test, using monthly mean data as the input. The approximate p-value threshold, p_fdr, area mean and standard deviation (over land only) are recorded in the map above.

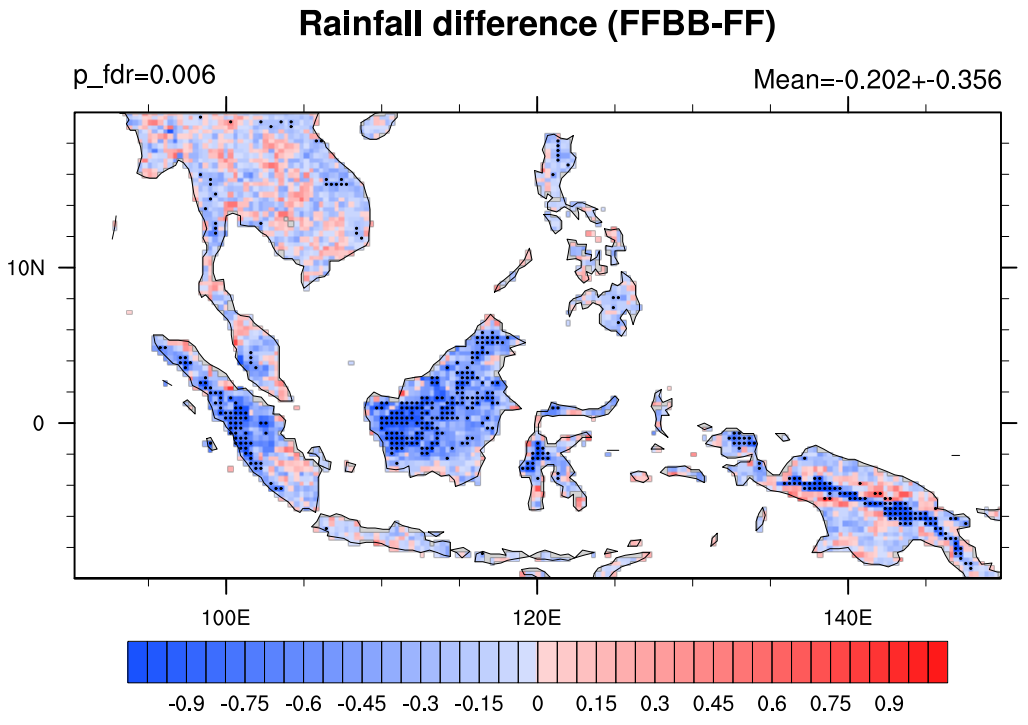

Figure S11. Total monthly mean precipitation differences (mm day^{-1}) between FFBB and FF simulations during 2002–2008. Black dot indicates differences that are statistically significant at a significance level of α_{fdr} = 0.05 after controlling the false discovery rate (FDR) (Benjamini and Hochberg, 1995; Wilks, 2016). The two-tailed p values are generated by Welch's t test, using monthly mean data as the input. The approximate p value threshold, p_fdr, and area mean and standard deviation (over land only) are written in above the map.

Reference

Allwine, K. J., and Whiteman, C. D.: Single-station integral measures of atmospheric stagnation, recirculation and ventilation, Atmospheric Environment, 28, 713-721, http://dx.doi.org/10.1016/1352-2310(94)90048-5, 1994.

Benjamini, Y., and Hochberg, Y.: Controlling the False Discovery Rate: A Practical and Powerful Approach to Multiple Testing, Journal of the Royal Statistical Society. Series B (Methodological), 57, 289-300, 1995.

Berg, P., Moseley, C., and Haerter, J. O.: Strong increase in convective precipitation in response to higher temperatures, Nature Geosci, 6, 181-185, http://www.nature.com/ngeo/journal/v6/n3/abs/ngeo1731.html - supplementary-information, 2013.

Malaysia, D. o. E.: A Guide To AIr Pollutant Index in Malaysia, 4 ed., edited by: Malaysia, D. o. E., 18 pp., 2000.

Wang, C.: Anthropogenic aerosols and the distribution of past large-scale precipitation change, Geophysical Research Letters, 42, 10,876-810,884, 10.1002/2015GL066416, 2015.

Wilks, D. S.: "The Stippling Shows Statistically Significant Grid Points": How Research Results are Routinely Overstated and Overinterpreted, and What to Do about It, Bulletin of the American Meteorological Society, 97, 2263-2273, 10.1175/BAMS-D-15-00267.1, 2016.